

**JAERI - M**  
**94-073**

**HEAT REMOVAL CAPABILITY OF  
DIVERTOR COAXIAL TUBE ASSEMBLY**

May 1994

Masanao SHIBUI, Masataka NAKAHIRA  
Eisuke TADA and Hideyuki TAKATSU



Heat Removal Capability of Divertor Coaxial Tube Assembly

Masanao SHIBUI, Masataka NAKAHIRA<sup>+</sup>  
Eisuke TADA<sup>+</sup> and Hideyuki TAKATSU

Department of ITER Project  
Naka Fusion Research Establishment  
Japan Atomic Energy Research Institute  
Naka-machi, Naka-gun, Ibaraki-ken

(Received March 31, 1994)

To deal with high power flowing in the divertor region, an advanced divertor concept with gas target has been proposed for use in ITER/EDA. The concept uses a divertor channel to remove the radiated power while allowing neutrals to recirculate. Candidate channel wall designs include a tube array design where many coaxial tubes are arranged in the toroidal direction to make louver. The coaxial tube consists of a Be protection tube encases many supply tubes wound helically around a return tube. V-alloy and hardened Cu-alloy have been proposed for use in the supply and return tubes. Some coolants have also been proposed for the design including pressurized He and liquid metals, because these coolants are consistent with the selection of coolants for the blanket and also meet the requirement of high temperature operation.

In the coaxial tube design, the coolant area is restricted and brittle Be material is used under severe thermal cyclings. Thus, to obtain the coaxial tube with sufficient safety margin for the expected fusion power excursion, it is essential to understand its applicability limit.

The paper discusses heat removal capability of the coaxial tube and recommends some design modifications.

Keywords: Gas Divertor, Divertor Channel, Liquid Metal, Be, Vanadium

---

<sup>+</sup> Department of Fusion Engineering Research

## ダイバータ用同軸集合管の除熱能力

日本原子力研究所那珂研究所ITER開発室

渋井 正直・中平 昌隆<sup>\*</sup>・多田 栄介<sup>\*</sup>・高津 英幸

(1994年3月31日受理)

ITER EDAでは、大パワーを扱う必要性からガス・ダイバータが提案されている。この概念には中性ターゲット粒子を再循環し、かつ、放射・散逸される熱を除去するためのチャンネル部が必要であり、このチャンネル壁の設計として、同軸管をトロイダル方向に配列したルーバ状のものが提案されている。同軸管は、冷却材戻り管のまわりに多数の供給管をヘリカル状に配し、これをBe製の保護管に収納したものである。給排管の材料にはバナジウム合金や強化銅が考えられている。また、冷却材としては、ブランケットの冷却構想と一致し、高温運転にも適したものである。ことで高圧Heや液体金属が提案されている。

同軸管を用いた設計では、冷却断面積が小さくなり、かつ、延性が小さいBe材が過酷な熱サイクルのもとで使用される。このため、予想される過出力に対して十分な裕度をもった同軸管を得るためにはその適用限度を知る必要がある。

本報告では、同軸管の除熱能力を調べ、若干の設計改善を提案する。

## Contents

1. Introduction .....	1
2. Coaxial Tube Design for ITER Divertor .....	1
2.1 Design Specifications .....	1
2.2 Outline of Coaxial Tube Design .....	2
3. Heat Removal Capability of He Cooled Coaxial Tube .....	2
3.1 Sensitivity Analysis .....	2
3.2 Numerical Results .....	4
3.3 Temperature Sharing of Component Parts .....	5
4. Thermal Stress in Be Tube .....	7
4.1 Thermal Stress Analyses .....	7
4.2 Numerical Examples .....	10
5. Conclusions .....	12
References .....	12

## 目    次

1. 序    言 .....	1
2. 同軸集合管構造に基づくITER用ダイバー設計 .....	1
2.1 設計仕様 .....	1
2.2 同軸集合管構造ダイバータ設計の概要 .....	2
3. ヘリウム冷却による除熱特性 .....	2
3.1 感度解析 .....	2
3.2 数値解析結果 .....	4
3.3 温度分布 .....	5
4. ベリリウム管内の熱応力 .....	7
4.1 熱応力解析 .....	7
4.2 数値解析例 .....	10
5. 結    言 .....	12
参考文献 .....	12

## 1. Introduction

To deal with high power flowing in the divertor region, an advanced divertor concept with gas target has been proposed for use in ITER/EDA[1,2]. In this concept, a divertor channel is required to remove the radiated power while allowing neutrals to recirculate. One of the candidate channel designs satisfying these requirements is a tube array design[1] where many coaxial tubes are arranged in the toroidal direction to make louver. The coaxial tube consists of a Be protection tube encases many supply tubes wound helically around a return tube. The coolant flows into the helical tubes and returns through the inner tube. V-alloy and hardened Cu-alloys have been proposed for use as the supply/return tube materials[2].

Some coolants have also been proposed including pressurized He and liquid metals, because these coolants meet the requirement of high temperature operation and also are consistent with the selection of coolants for the blanket. The He cooled option, although some of the safety issues can be solved because of its inherent safety nature, high pressure operation ( $\sim 20\text{MPa}$ ) will be necessary. Cooling with liquid metals may allow low pressure operation. However, new technology must be developed on the formation of a self healing electrical insulation to reduce the MHD effects.

In the coaxial tube design, coolant area is restricted and brittle Be material is used under severe thermal cyclings. Thus, to obtain the tube with sufficient safety margin for the expected fusion power excursion, it is essential to understand its performance limit.

The paper discusses heat removal capability of the coaxial tube and recommends some design modifications.

## 2. Coaxial Tube Design for ITER Divertor

### 2.1 Design specifications

Because of uncertainty in power sharing between divertor and first wall, the divertor is to be designed to safely handle 80% of  $\alpha$ -power[1]. For 3 Gw normal operation, this condition enables to estimate a peak heat flux of  $3\text{ Mw/m}^2$  on the divertor channel wall. Since the divertor is required to withstand power excursion, the following values are specified as design guideline[1]:

- Length between x-point and back plate = 2 m (IB), 2.5 m (OB),
- Power input = 480 Mw by radiation/charge exchange(80% of  $\alpha$ -power),  
 $\sim 100\text{ Mw}$  as nuclear heating,

- Surface material/temperature = Be/300-800°C.
- Peak design heat load on channel wall  $\leq 5 \text{ Mw/m}^2$ ,
- Design neutron damage  $\leq 5 \text{ dpa}$ .
- Temperature between pulses  $\geq 200^\circ\text{C}$ .

## 2.2 Outline of coaxial tube design

The divertor proposed in the report[1] consists of five modules per  $15^\circ$  toroidal sector. Each module has shield structure and coaxial tubes arranged to make channel walls as schematically shown in Fig.2.1. The total height of the divertor module is about 2.2 m, whereas its toroidal width is about 0.5 m. Each coaxial tube consists of a Be protection tube which contains many V-alloy tubes helically wound around a V-alloy inner tube. One example design is presented in Fig.2.2, showing the coaxial tube design with ten helical tubes cooled with the pressurized He gas (20MPa). Gaps between component parts are filled with liquid metal (Li or Na) to make compliant layers while achieving good heat conduction. The Be protection tube having an outer diameter of about 46 mm is designed not to be a pressure boundary for the coolant.

The He gas with an inlet temperature of over  $200^\circ\text{C}$  is supplied from the helical tubes and extracted from the inner tube. It should be noted that the coaxial design also allows the use of a liquid metal as an coolant, if the self healing electrical insulation is successfully made on the inner surface of cooling tubes. Hot water may also be introduced when it is selected as the coolant for the blanket.

## 3. Heat Removal Capability of He Cooled Coaxial Tube

### 3.1 Sensitivity analysis

Fig.3.1 shows the analytical model to examine heat removal capability of the coaxial tube. The model includes ten parameters which are:

- Number of supply tubes :  $N$ ,
- Outer radius and wall thickness of supply tube :  $r_s$ ,  $t_s$ ,
- Outer radius and wall thickness of return tube :  $r_r$ ,  $t_r$ ,
- Outer radius and average wall thickness of outer tube :  $r_o$ ,  $t_o$ ,
- Gap between component parts :  $g$ ,
- Coolant velocity in supply tube :  $V_s$ ,
- Heated length of coaxial tube :  $L_w$ .

Wall thickness of the component tubes may be determined either from the primary stress limit or from the minimum thickness requirement in the welding process for a high pressure application. Here, because of difficulties in the non-destructive testing after assembly, any tube is assumed to have at least 2 mm wall thickness. Thus,

$$t_1 = F_v r_1, \quad t_2 = F_B r_2, \quad t_3 = F_v r_3, \\ \text{if } t_n, n=1-3, \geq 2 \text{ mm.} \quad (3.1)$$

where

$$F_v = P_{He} / S_v, \quad F_B = P_{Li} / S_B, \quad (3.2)$$

$P_{He}$  = pressure of He coolant (=20 MPa),

$P_{Li}$  = pressure of liquid Li (=0.1 MPa),

$S_v$  = allowable stress of V-alloy,

$S_B$  = allowable stress of Be.

From geometrical considerations (see Fig. 3.1),

$$r_1 + 2(g + r_2) + t_3 - r_2 = 0, \quad (3.3a)$$

$$g + r_2 \leq r_1 \cdot \sin(\pi/N) / \{1 - \sin(\pi/N)\}. \quad (3.3b)$$

Maximum temperature rises of He gas and Be tube are given by :

$$\Delta T_{He} = 2r_2 L h q_s / \{(r_2 - t_3)^2 \pi \rho C_p V_s N\}, \quad (3.4)$$

$$\Delta T_{Be} = \Delta T_{He} + q_s \{t_3 / \kappa_v + (\delta - r_2 - g) / \kappa_B + 1/h + g / \kappa_L\}, \quad (3.5)$$

respectively, where

$$\delta = (r_2^2 - 2r_2(r_1 + g + r_2) \cos(\pi/N) + (r_1 + g + r_2)^2)^{1/2}, \quad (3.6)$$

and

$\Delta T_{He}$  = maximum temperature rise of He coolant,

$\Delta T_{Be}$  = maximum temperature rise of Be tube,

$q_s$  = surface heat flux,

$\rho C_p$  = heat capacity of He coolant,

$h$  = heat transfer coefficient on the inner surface of supply tubes,

$\kappa_v, \kappa_B, \kappa_L$  = thermal conductivity of V-alloy, Be and Li, respectively.

Heat transfer coefficient is calculated from the Nusselt number given by[3]:

$$Nu = (C_r/2) Re Pr (1 - 1000/Re) / \{1 + 12.7(C_r/2)^{1/2} (Pr^{2/3} - 1)\} \quad (3.7)$$

where Re is the Reynolds number, Pr is the Prandtl number and

$$C_r = (1.58 \cdot \log Re - 3.28)^{-2}.$$

Under the assumption of constant thermohydraulic parameters, the pressure drop in

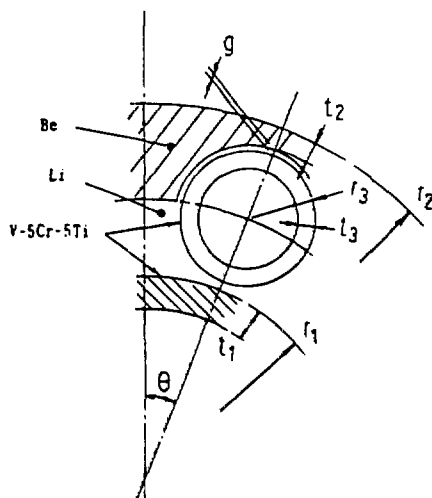


Fig. 3.1 Analytical model



the divertor region is estimated from the equation:

$$\Delta P = \Delta P_{i,s} + \Delta P_s + \Delta P_r + \Delta P_c. \quad (3.8)$$

where

$\Delta P_{i,s}$  = pressure drop at the entrance of the supply tube ( $=\rho V_s^2/2$ ).

$\Delta P_s$  = pressure drop in the supply tube ( $=\lambda_s(L_s/2(r_s-t_s))\rho V_s^2/2$ ).

$\Delta P_r$  = pressure drop in the return tube ( $=\lambda_r(L_r/2(r_r-t_r))\rho V_r^2/2$ ).

$\Delta P_c$  = pressure drop due to velocity change ( $=\rho(V_s-V_r)^2/2$ ).

and  $V_r$  is the coolant velocity in the return tube,  $\rho$  is the density of coolant,

$\lambda_s$  and  $\lambda_r$  are friction factors for the supply and return tubes, respectively.

Here  $\lambda_s$  is calculated from the equation [3]:

$$\lambda_s = (0.029 + 0.304(\text{Re}(a/R))^2)^{-1/4} (a/R)^{1/2}, \quad (3.9)$$

where

$$a = r_s - t_s, \quad R = R_0(1 + (L_0/2\pi R_0)^2), \quad R_0 = r_1 + r_2, \quad (3.10)$$

and  $L_0$  is the helical pitch. To estimate  $\lambda_r$  for a straight tube, the empirical equation proposed by White[4] is used.

For the commercially available Be blocks (cross rolled or hot pressed block), elongation decreases at temperature higher than 500°C[5], and compatibility with liquid metals (Na and Li) is poor at temperature above 500-600°C[5]. In addition, under the ITER irradiation condition, swelling of Be materials may become serious at temperature higher than 600°C[6]. Here the applicable temperature of the Be tube is assumed to be 500°C. This condition gives

$$\Delta T_{b,s} + T_{b,s} \leq T_{lim}, \quad (3.11)$$

where

$T_{b,s}$  = base temperature,

$T_{lim}$  = 500°C.

The present problem includes 10 parameters. Two of them,  $r_2$  and  $L_m$ , may be determined from the divertor physics considerations and, therefore, are treated as given parameters, i. e.,  $r_2=22.5$  mm (cf. Fig.2.2) and  $L_m=1.5$  m as reported in [1]. Since eqs. (3.1), (3.3)-(3.5) and (3.8) include 8 equations for solving 8 unknowns, sensitivity analyses for any interesting parameter can be performed systematically.

### 3.2 Numerical results

Table 3.1 presents thermo-mechanical properties of divertor materials used in the present analyses.

Numerical results are shown in Figs.3.2 and 3.3 where  $\Delta T_{b,s}$ ,  $\Delta P$ ,  $V$ , and tube

dimensions are presented as a function of the He supply velocity  $V_s$ . In these figures, only the results are shown for  $V_s$  below 200 m/s, because the higher velocity is considered to be unrealistic. It should be noted that there exists no solution satisfying eqs. (3.3) and (3.4) in the unplotted lower  $V_s$  region.

Fig. 3.2 presents the results for the heat loading of  $5 \text{ Mw/m}^2$ , showing that  $\Delta T_{\text{Be}}$  exceeds  $1000^\circ\text{C}$  even when  $\Delta T_{\text{He}}=150^\circ\text{C}$  and  $V_s=200 \text{ m/s}$ . Since this temperature rise is too high compared with  $T_{\text{lim}}$  (eq. (3.11)), it may be concluded that there will be no practical solution for handling the heat load of  $5 \text{ Mw/m}^2$ -1.5 m with the He cooled coaxial tube.

The results for  $2 \text{ Mw/m}^2$ -1.5 m are presented in Fig. 3.2 where  $\Delta T_{\text{He}}$  is fixed to be  $150^\circ\text{C}$ . In this case,  $\Delta T_{\text{Be}}$  below  $600^\circ\text{C}$  is achieved at  $V_s=100 \text{ m/s}$ . However, this is still high, because  $T_{\text{lim}}=500^\circ\text{C}$ .  $\Delta T_{\text{Be}}$  is not so sensitive to  $V_s$ , implying that the design with high  $V_s$  is not necessarily effective method for reducing  $\Delta T_{\text{Be}}$ . Although the 10 supply tube design gives lower  $\Delta T_{\text{Be}}$  than the 8 tube design, its solution window is narrow in the low velocity region of  $V_s < 100 \text{ m/s}$ .

Table 3.1 Thermo-mechanical properties of divertor materials

Property		He	Be	V5Cr5Ti	Li	Water
Density	$\rho$ [kg/m <sup>3</sup> ]	15.4				762
Specific heat	$C_p$ [KJ/KG-K]	5.19				5.14
Thermal cond.	$\kappa$ [w/mK]	0.286	126 <sup>1)</sup>	30.7	45.8	0.589
Prandtl number	Pr	0.652				0.896
K. Viscosity	$\nu$ [ $\mu\text{m}^2/\text{s}$ ]	2.7				0.126
Allowable Str.	S [MPa]		51 <sup>2)</sup>	140		

1) At about  $400^\circ\text{C}$ [5].

2) 1/3 of tensile strength at  $600^\circ\text{C}$ [5].

### 3.3 Temperature sharing of component parts

The maximum temperature of the Be tube is the summation of temperature differences in the component parts and, from eq. (3.10), this is given by

$$\text{Max. } T_{\text{Be}} = T_{\text{He}} + \Delta T_c + \delta T_f + \delta T_v + \delta T_{L1} + \delta T_{\text{Be}} \quad (3.11)$$

where

$\Delta T_c$  = temperature rise of coolant (=  $\Delta T_{\text{He}}$  for He cooled design),

$\delta T_f$  = film temperature difference (=  $q_s/h$ ).

$\delta T_v$  = temperature difference in supply tube wall ( $=q_s t_s / \kappa_v$ ).

$\delta T_{L1}$  = temperature difference in gap ( $=q_s g / \kappa_g$ ).

$\delta T_{Be}$  = temperature difference in Be tube wall ( $=q_s (\delta - r_s - g) / \kappa_{Be}$ ).

To understand temperature sharing of component parts, the He cooled coaxial design with  $r_s = 2.7$  mm,  $t_s = 1.1$  mm and  $N = 10$  [1] are examined under the assumption of no volumetric heat load. Results are summarized in table 3.2 along with those for the water cooled option. In the table, temperature differences can be normalized with the surface heat flux  $q_s$ , because nonlinear effects and volumetric heat load are neglected. For example, when  $q_s = 2$  Mw/m<sup>2</sup>, Max.  $T_{Be} = 508^\circ\text{C}$  for the water cooled design with  $V_s = 5$  m/s.

Table 3.2 Temperature sharing in coaxial design

Item	He (20 MPa)			Water (10 MPa)		
$q_s$ [Mw/m <sup>2</sup> ]	5			5		
$V_s$ [m/s]	100	150	200	3	5	10
$h$ [ $10^4$ w/m <sup>2</sup> K]	1.64	2.27	2.85	2.49	4.26	7.41
$T_{Be}$ [°C]	250	←	←	250	←	←
$\Delta T_c$	185	123	92	125	75	38
$\delta T_r$	305	221	175	200	118	68
$\delta T_v$ (1.1 mm)	179	←	←	179	←	←
$\delta T_{L1}$ (0.7 mm)	77	←	←	77	←	←
$\delta T_{Be}$ (4.95 mm <sup>1</sup> )	197	←	←	197	←	←
Max. $T_{Be}$ [°C]	1193	1047	970	1028	896	809
$(\Delta T_c + \delta T_r) / \text{Max. } T_{Be}$	0.41	0.33	0.28	0.32	0.22	0.13
$T_{Be} / \text{Max. } T_{Be}$	0.21	0.24	0.26	0.24	0.28	0.31

( ) : Heat conduction length.

1) : Actual heat conduction length given by eq. (3.6).

Contribution of  $\delta T_v$  to Max.  $T_{Be}$  is small compared with that of  $\delta T_{Be}$  in the design with 1.1 mm thick vanadium and 4 mm thick Be tubes. However, when a wall thickness of 2 mm is required in the welding process,  $\delta T_v$  will be about 1.8 times that listed in table 3.2 and also  $\Delta T_c$  will be 2.25 times as high as the listed value because the coolant area is reduced. This implies that use of materials with high thermal conductivity is necessary for the supply tubes. For example, when the

V-alloy is replaced with DSC, the temperature difference in the supply tube wall can be reduced by more than 100°C.

The base temperature  $T_{b,0}$  takes about 20 ~ 30% of  $Max.T_{b,0}$ , and therefore, it will limit applicability of the coaxial tube design. This may be true, because available temperature margin of Be reduces when  $T_{b,0}$  is high. In the present case, the temperature margin is 250°C when  $T_{b,0}=500°C$ . The corresponding allowable heat flux is estimated to be 1.3  $Mw/m^2$  for the He cooled option with  $V_c=100$  m/s and 1.9  $Mw/m^2$  for the water cooled option with  $V_c=5$  m/s.

Since the value,  $\Delta T_c + \delta T_c$ , is a function of thermal properties of coolant, it may present one of the guidelines on the selection of coolant. In the interesting region of the coolant velocity,  $\Delta T_c + \delta T_c$  takes 30~40% of  $Max.T_{b,0}$  in the He cooled option and about 20% in the water cooled option. Therefore, although the tube design must be modified to meet safety requirements, the water cooled option is desirable.

#### 4. Thermal Stress in Be Tube

##### 4.1 Thermal stress analyses

In the coaxial tube design, the gap between the supply tubes and the Be tube is filled with liquid metal to make the compliant layer. Therefore, the Be tube is expected to behave independently under heat loadings. This situation may allow to analyze only the Be tube with suitable assumption on heat transfer at its inner surface.

Here the two dimensional problem is analyzed where a Be tube is subjected to surface and volumetric heat loads and is cooled uniformly from its inner surface. For simplicity, temperature dependence of material properties and the thermal stress due to uniform temperature rise are neglected here.

In two dimensional steady state heat flow shown in Fig. 4.1, the temperature rise  $T$  satisfies the equation:

$$T, z\bar{z} = -q_0/4\lambda \quad (4.1)$$

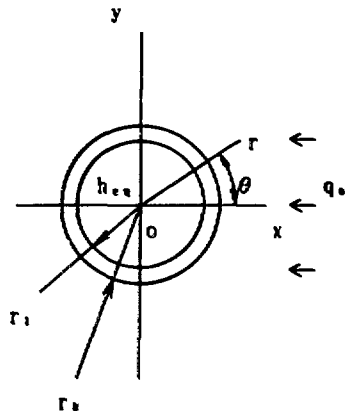


Fig.4.1 Analytical model

where

$q_v$  = volumetric heat load,

$\lambda$  = thermal conductivity,

$z = x + iy$  ( $= r \cdot \exp(i\theta)$ ),

$i = \sqrt{-1}$ ,

and  $T, z\bar{z} = \partial^2 T(z, z) / \partial z \partial \bar{z}$ .

The boundary conditions are

$$(\lambda / r)(zT, z + \bar{z}T, \bar{z}) = q \quad \text{on } z = r_2, \quad (4.2a)$$

$$(\lambda / r)(zT, z + \bar{z}T, \bar{z}) = h_{e,e}T \quad \text{on } z = r_1, \quad (4.2b)$$

where

$$q = q_v \left\{ 1/2 - (2/\pi) \sum_{n=1}^{\infty} (-1)^n \frac{\cos(2n-1)\theta}{2n-1} \right\}. \quad (4.3)$$

and

$r_1, r_2$  = inner and outer radii, respectively,

$h_{e,e}$  = equivalent heat transfer coefficient,

$q_v$  = surface heat flux.

Eq. (4.1) with eq. (4.2) can easily be solved to yield:

$$T = \sum_{n=1}^{\infty} a_n \{ z^{2n-1} + \bar{z}^{2n-1} + \xi_n (z^{-2n+1} + \bar{z}^{-2n+1}) + a_0 \log(z\bar{z}/r_1^2) - q_v z\bar{z}/4\lambda + \xi_0 \}. \quad (4.4)$$

where

$$a_n = - \frac{q_v}{\pi \lambda} \frac{(-1)^n}{(2n-1)^2} \frac{r_2^{2n}}{r_2^{4n-2} - \xi_n}, \quad \xi_n = r_1^{4n-2} \frac{1 - r_1 h_{e,e} / \lambda (2n-1)}{1 + r_1 h_{e,e} / \lambda (2n-1)},$$

$$a_0 = (r_2 / 4\lambda) (q_v r_2 + q_v),$$

$$\xi_0 = (q_v / 2h_{e,e} r_1) (r_2^2 - r_1^2 + r_1^2 h_{e,e} / 2\lambda) + q_v r_2 / 2h_{e,e} r_1.$$

The equivalent heat transfer coefficient  $h_{e,e}$  may be defined by:

$$h_{e,e} = 1.0 / \{ 1/h + t_s / (\eta \kappa_v) + g / \kappa_L \} \quad (4.5)$$

where  $\eta$  is the averaging factor introduced to account for the arrangement of the supply tubes. For the tube design with V-alloy, it may be difficult to achieve high  $h_{e,e}$ . For example,  $h_{e,e} = 8.9 \times 10^3$  w/m<sup>2</sup>K when  $h = 4 \times 10^4$  w/m<sup>2</sup>K,  $\eta = 1.0$ ,  $t_s = 2$  mm and  $g = 1$  mm. However, when V-alloy is replaced with Cu-alloy (DSC, 288 w/mK),  $h_{e,e} = 1.9 \times 10^4$  w/m<sup>2</sup>K for the same condition.

The maximum temperature rise occurs at  $z=r_2$  and is given by

$$T_m = -\frac{2q_0 r_2}{\pi \lambda} \sum_{n=1}^{\infty} \frac{(-1)^n}{(2n-1)^2} \frac{1 + \xi_n / r_2^{4n-2}}{1 + \xi_n / r_2^{4n-2}} + 2a_0 \log(r_2/r_1) - q_0 r_2^2 z z / 4 \lambda + \xi_0 \quad (4.6)$$

The thermal stresses can be obtained by the superposition method[7]. The method requires the thermoelastic displacement potential  $f$  defined by the particular solution of the following equation:

$$f, z\bar{z} = \beta \alpha T \quad (4.7)$$

where

$\beta = (1 + \nu) / 4(1 - \nu)$  for plane strain problem,

$\alpha$  = coefficient of thermal expansion,

$\nu$  = Poisson's ratio.

Stress and displacement components are obtained from the equations:

$$\sigma_R + i \tau_{R\tau} = \phi' + \bar{\phi}' - z\bar{\phi}'' - (\bar{z}/z) \bar{\chi}' - 4G \{f, z\bar{z} - (\bar{z}/z) f, \bar{z}\bar{z}\} \quad (4.8a)$$

$$\sigma_T - i \tau_{R\tau} = \phi' + \bar{\phi}' + z\bar{\phi}'' + (\bar{z}/z) \bar{\chi}' - 4G \{f, z\bar{z} + (\bar{z}/z) f, \bar{z}\bar{z}\} \quad (4.8b)$$

$$\sigma_z = 2\nu (\phi' + \bar{\phi}') - 8Gf, z\bar{z} \quad (4.8c)$$

$$2G(u_R + i u_T) = \exp(-i\theta) (\kappa \phi - z\bar{\phi}' - \bar{\chi} + 4Gf, \bar{z}) \quad (4.9)$$

where

$\sigma_R, \sigma_T, \tau_{R\tau}$  = polar stress components,

$\sigma_z$  = axial stress,

$u_R, u_T$  = polar displacement components,

$\phi, \chi$  = complex potentials,

$\kappa = 3 - 4\nu$  for plane strain,

$G$  = shear modulus,

and  $\phi' = d\phi(z)/dz$ , for example.

The boundary conditions for the present problem are:

$$\sigma_R + i \tau_{R\tau} = 0 \text{ on } r=r_1, r_2 \quad (4.10)$$

The displacement components given by eq. (4.9) must be single-valued. Using this condition and eq. (4.10),  $\phi$  and  $\chi$  are easily obtained in the form of a polynomial. Consequently,

$$\sigma_R + i \tau_{R\tau} = 2(b_0 + b_1 z) + (e_0 + 2e_1/\bar{z})/z\bar{z} + 4G\alpha\beta [a_0 \{1 - \log(z\bar{z}/r_1^2)\} - a_1 (z + 2\xi_1/\bar{z}) + q_0 z\bar{z}/8\lambda - \xi_0] \quad (4.11a)$$

$$\sigma_T - i \tau_{R\tau} = 2b_0 + 2b_1 (z + 2\bar{z}) - (e_0 + 2e_1/\bar{z})/z\bar{z} + d_0/z - 4G\alpha\beta [a_0 \{1 + \log(z\bar{z}/r_1^2)\} + a_1 (z + 2\bar{z} + \xi_1/z) - 3q_0 z\bar{z}/8\lambda + \xi_0] \quad (4.11b)$$

where

$$d_0 = -4G\alpha\beta a_1 \xi_1$$

$$e_0 = 4G\alpha\beta r_1^2 (q_0 r_2^2 / 8\lambda - 2a_0 \log(r_2/r_1) / (1 - r_1^2/r_2^2)),$$

$$2b_0 = -e_0/r_1^2 - 4G\alpha\beta (a_0 - \xi_0 + q_0 r_1^2 / 8\lambda),$$

$$e_1 = 4G\alpha\beta a_1 \xi_1 r_1^2 / (1 + r_1^2/r_2^2),$$

$$b_1 = 2G\alpha\beta a_1 (1 + 2\xi_1/r_1^2) - e_1/r_1^4.$$

$\sigma_r$  on  $\theta = 0$  is a key stress distribution for the failure analysis, because  $\sigma_r$  at  $z = r_1$  is positive. This is given by

$$\sigma_r(\theta = 0) = 6b_1 r + 2b_0 - (e_0 + 2e_1/r) / r^2 + d_0/r - 4G\alpha\beta [a_0 (1 + 2 \log(r/r_1)) + a_1 r (3 + \xi_1/r^2) - 3q_0 r^2 / 8\lambda + \xi_0]. \quad (4.12)$$

It should be noted that the axial stress given by eq. (4.8c) is induced only when the tube is restrained at its ends. Therefore, when the tube ends are free, the resultant axial force and moment calculated from eq. (4.8c) must be applied at its ends to maintain the plane strain condition. In this case, however, eqs. (4.11) still gives inplane stresses far away from the tube ends.

#### 4.2 Numerical examples

Thermo-mechanical properties of Be depend largely on the production process. In the present study, the typical properties listed in table 4.1 have been used.

Table 4.1 Thermo-mechanical properties of Be

Th. cond. $\lambda$ [W/mK]	C. T. E $\alpha$ [ $K^{-1}$ ]	Young's M. E [GPa]	P. R. $\nu$	Yield Str. $\sigma_y$ [MPa] <sup>1)</sup>		Tensile Str. $\sigma_u$ [MPa] <sup>1)</sup>	
600°C				500°C	600°C	500°C	600°C
106	$1.2 \times 10^{-6}$	231 <sup>2)</sup>	0.025	182	112	252	153

1) Extruded bar [5]

2) At 400°C for cross rolled plate or at 650°C for hot pressed block

The maximum temperature rise and thermal stress can be expressed in the forms:

$$T_m = B_0 q_0 + B_1 q_{0..} \quad (4.13a)$$

$$\sigma_r(z=r_1) / 4G\lambda\alpha\beta = A_0 q_0 + A_1 q_{0..} \quad (4.13b)$$

where  $B_0$ ,  $B_1$ ,  $A_0$  and  $A_1$  are magnification constants. Fig. 4.2 shows these constants as a function of radius ratio  $r_1/r_2$ . The constant  $A_1$  is almost linear in the region of  $r_1/r_2 > 0.7$ .

Fig. 4.3 shows  $T_m$  and  $\sigma_r(z=r_1)$  for the tube having  $r_2=23$  mm and a wall thickness of 3.45 mm, cooled with  $h_{c,0}=1 \times 10^4$  w/m<sup>2</sup>K. When  $q_0=5$  Mw/m<sup>2</sup>,  $\sigma_r(z=r_1)$  exceeds 200 MPa and  $T_m$  is about 750°C. When the base temperature is 250°C, the maximum temperature of the Be tube exceeds 1000°C which is much higher than  $T_{lim}$  (eq. (3.11)). It should be noted that for larger  $h_{c,0}$  higher in-plane stresses will be induced.

Fig. 4.4 shows temperature rise and thermal stress distributions in the Be tube subjected to heat loads of 5 Mw/m<sup>2</sup> and 15 Mw/m<sup>2</sup>, cooled with  $h_{c,0}=2 \times 10^4$  w/m<sup>2</sup>K. This cooling condition may be achieved in a water cooled Cu tube design with  $v_0=5$  m/s (see table 3.2)). The solid and broken lines are the results for the wall thickness of 3mm and 2mm, respectively. In the case of  $r_1/r_2=0.870$  ( $t=3$  mm for  $r_2=23$  mm), the maximum temperature rise is 440°C, giving the maximum temperature of 765°C when  $T_{b,0}=250$ °C and  $\Delta T_0=75$ °C (see table 3.2). This is higher than  $T_{lim}$ .

It can be understood from Fig. 4.4 that the bending stress dominates over the membrane stress. In the case of  $r_1/r_2=0.870$ , membrane and bending stresses are 10 MPa and 200 MPa, respectively. This stress level is high compared with yield stress of commercially available Be materials (see table 4.1). The reduction of wall thickness by 1mm results in the reduction of stress by about 75 MPa.

In the case of plane strain, the axial stress is given by eq. (4.8c) or by

$$\sigma_z = \nu (\sigma_n + \sigma_r) - \alpha ET. \quad (4.14)$$

Therefore, since  $\nu=0.025$ ,  $\sigma_z = -\alpha ET$ . For example,  $\sigma_n=0$ ,  $\sigma_r=210$  MPa and  $T=290$ °C at  $z=r_1$  for  $r_1/r_2=0.870$  (see Fig. 4.4). In this case, from eq. (4.14),  $\sigma_z = -800$  MPa and the corresponding equivalent Mises stress exceeds 920 MPa. Thus, it is recommended that the Be tube be used under the unrestrained condition at its ends.



## 5. Conclusions

The heat removal capability of the coaxial tube design has been discussed.

The results are summarized as follows:

- (1) There may be no practical solution for handling  $5 \text{ Mw/m}^2$ -1.5m with the coaxial tube design. When the heat load is reduced to  $2 \text{ Mw/m}^2$ -1.5m, a design window may exist for the water cooled design.
- (2) To obtain the coaxial tube with sufficient safety margin, base temperature must be reduced. In addition, use of high conductivity materials such as Cu-alloys is recommended for the supply tubes.
- (3) Temperature rise of the Be tube is not so sensitive to the coolant velocity. Therefore, the design with high coolant velocity is not necessarily effective method for reducing temperature rise of the Be tube.
- (4) The in-plane thermal stress field may be characterized by the dominant bending stress. Be materials with high ductility are required rather than with high yield strength.
- (5) It is recommended that the Be tube be used under the unrestrained condition where the axial stress is free at its ends. Use of straight tube with fixed one end will improve applicability limit of the coaxial tube design.

## References

- [1] P-H.Rebut, ITER Design Option Developments, Naka JCT, 9-11 Sep. 1993.
- [2] K. J. Dietz and P-H Rebut, Proc. of the 15th SOFE, Hyannis(1993)4-0B-2.
- [3] JSME Data Book : Heat Transfer 4th Ed., (1986)55.
- [4] JSME Data Book : Hydraulic Losses in Pipes and Ducts(1979)26.
- [5] 'Be', published by NKG Insulators Limited.
- [6] D. Smith, et. al., ITER IDS, No. 29(1991)236.
- [7] S. P. Timoshenko and J. N. Goodier, 'Theory of Elasticity', 3rd ed., McGraw-Hill Book Company(1970).

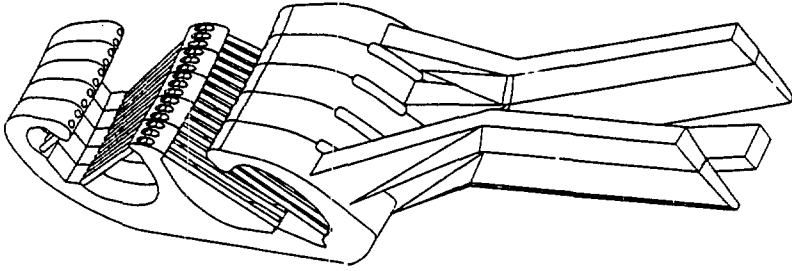


Fig. 2.1 Divertor module showing channel walls with coaxial tubes.

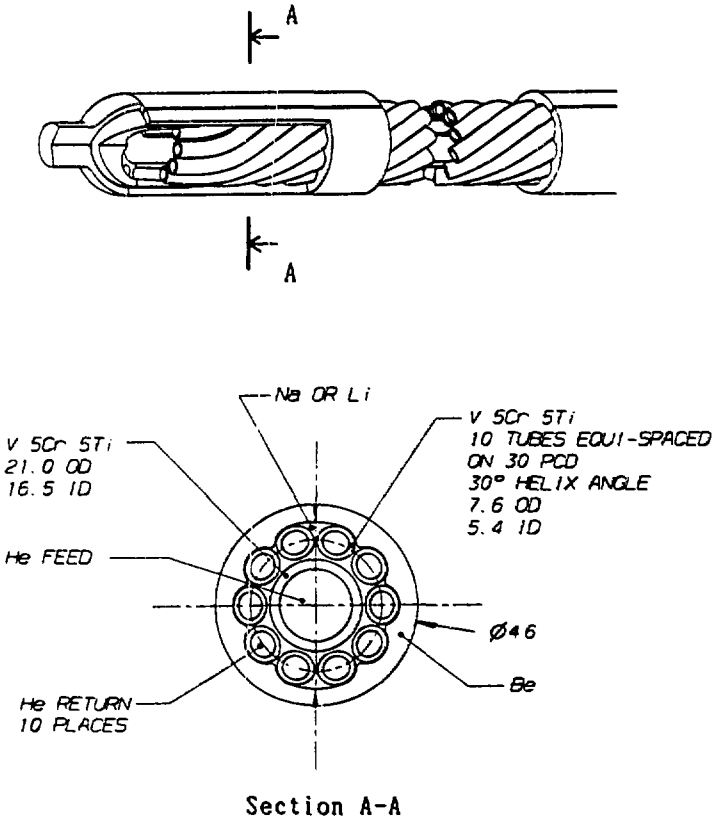


Fig. 2.2 Coaxial tube design with ten supply tubes wound helically around return tube.

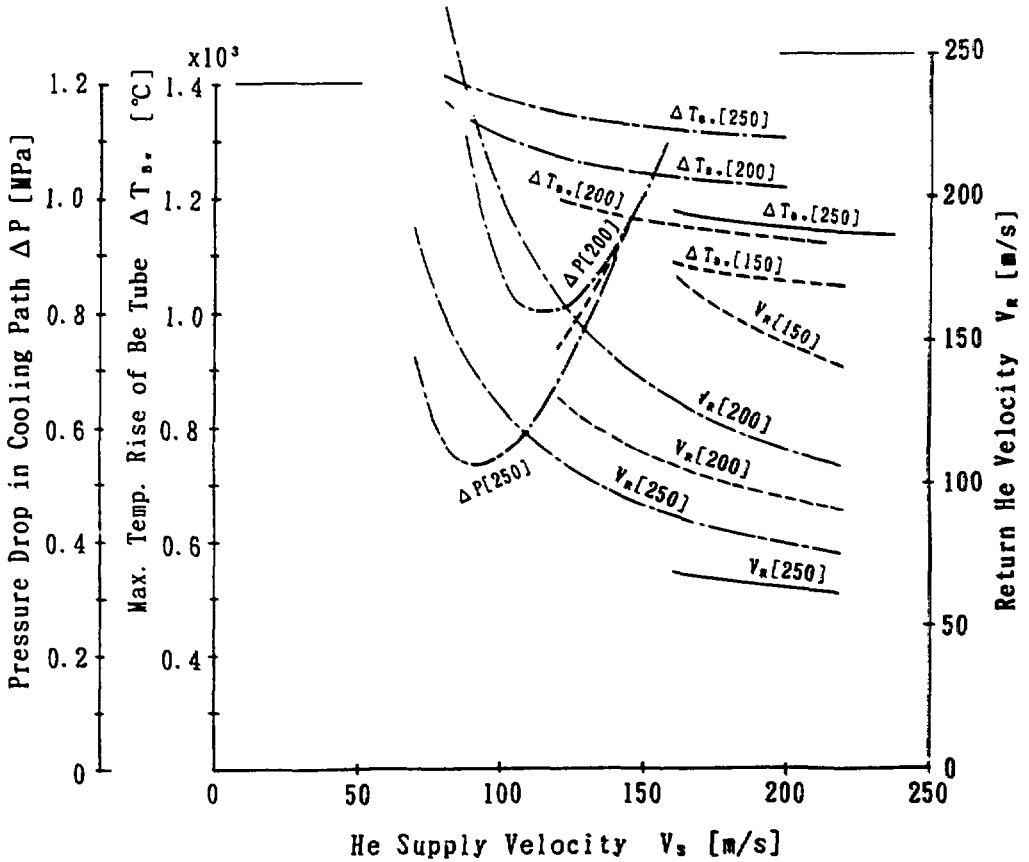
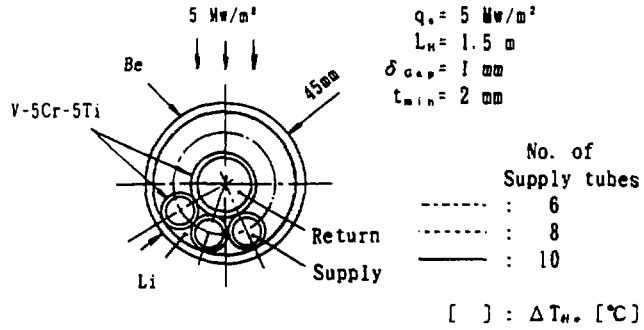


Fig. 3.2 Thermo-hydraulic performance of He cooled coaxial tube having an outer diameter of 45 mm.

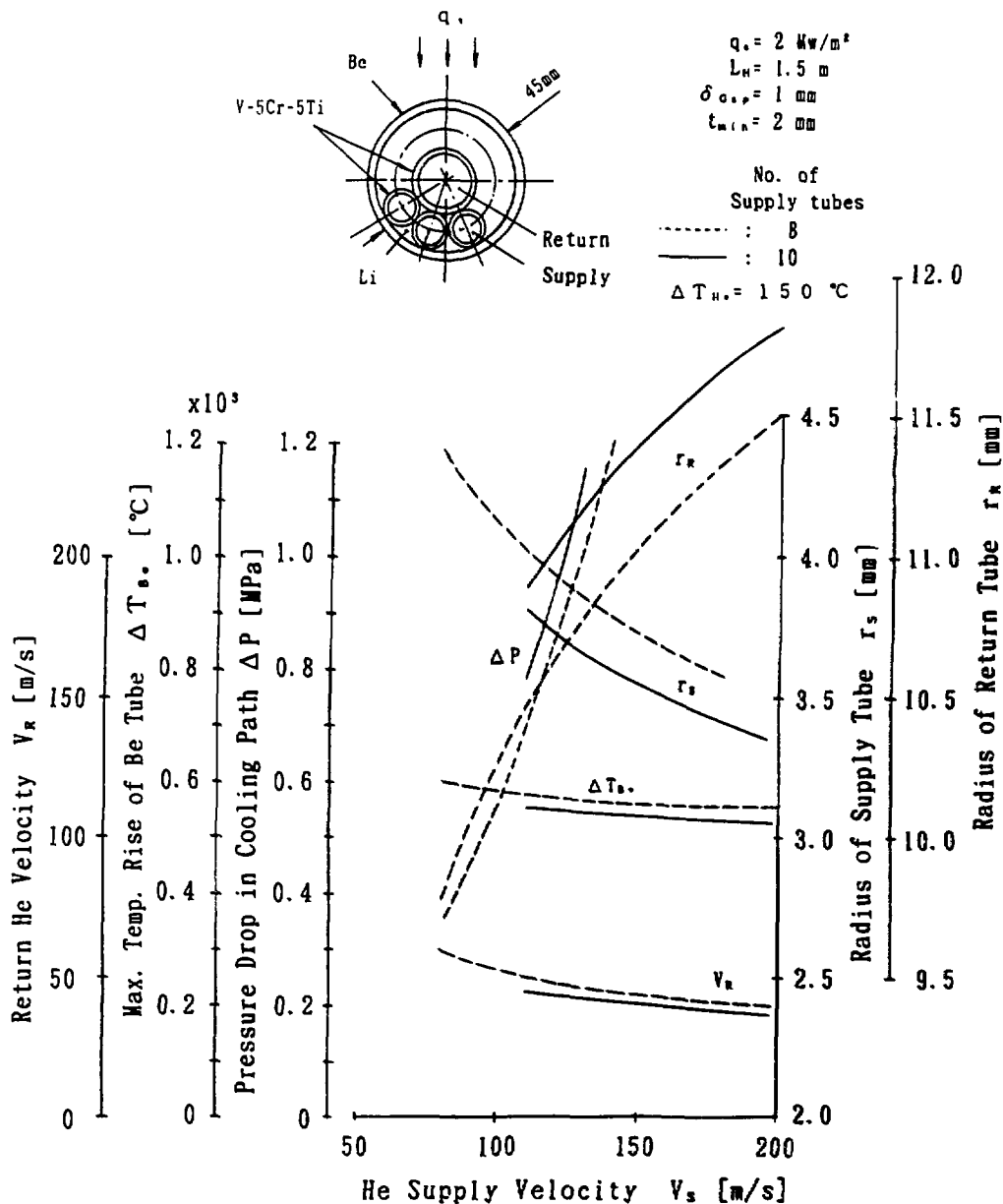


Fig. 3.3 Thermo-hydraulic performance of He cooled coaxial tube subjected to a surface heat flux of  $2 \text{ Mw/m}^2$ .

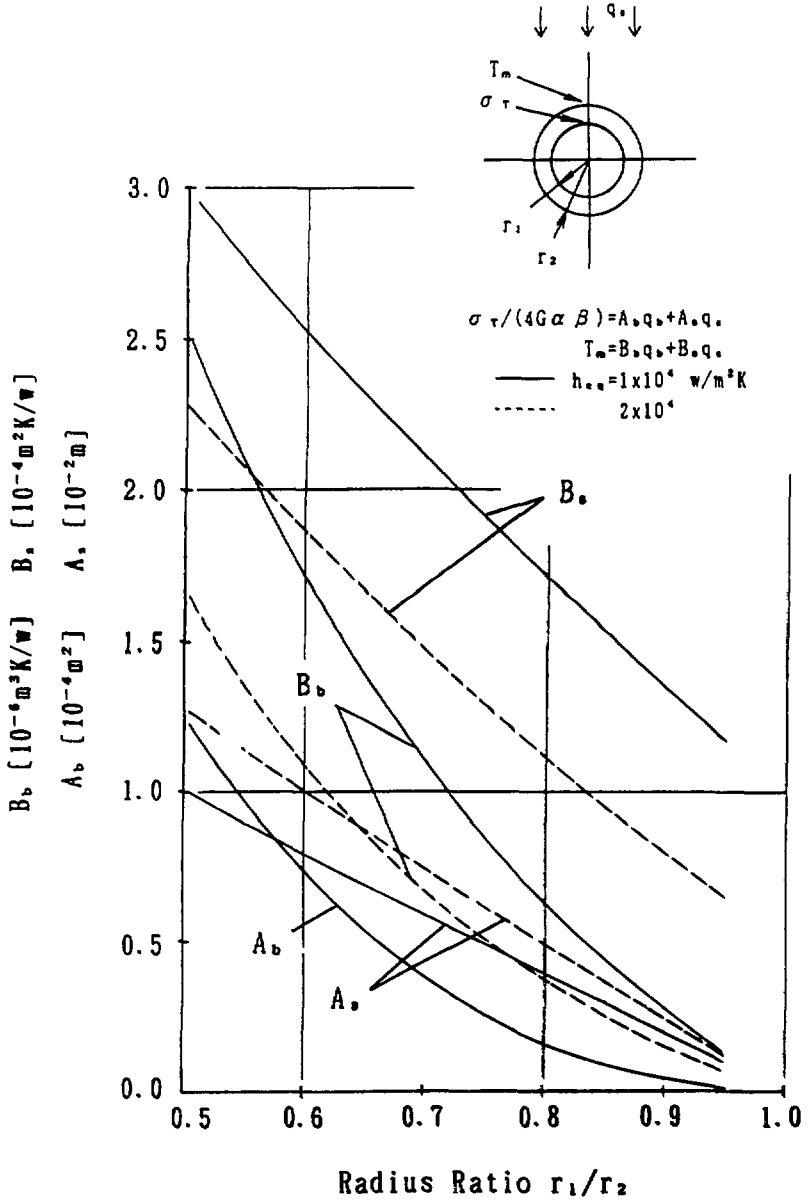


Fig. 4.2 Magnification constants as a function of radius ratio  $r_1/r_2$ .

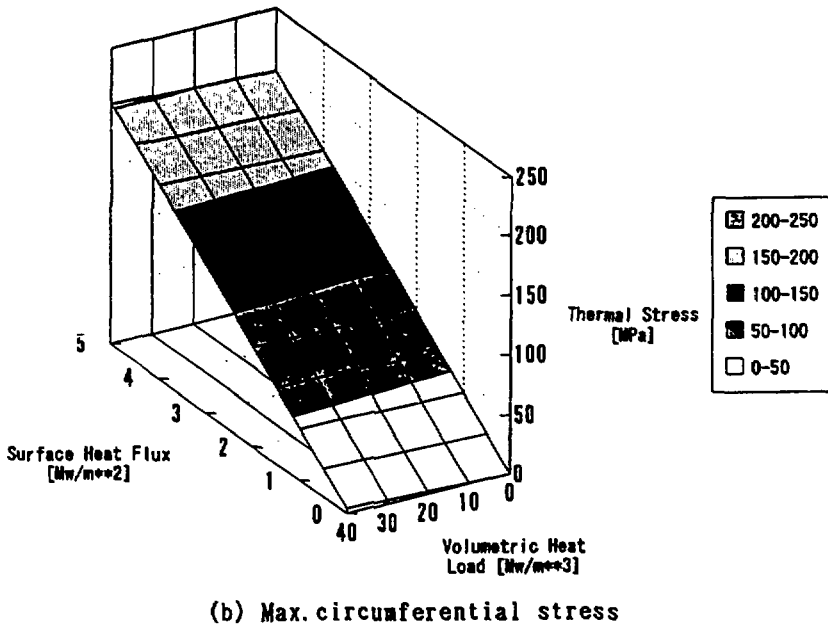
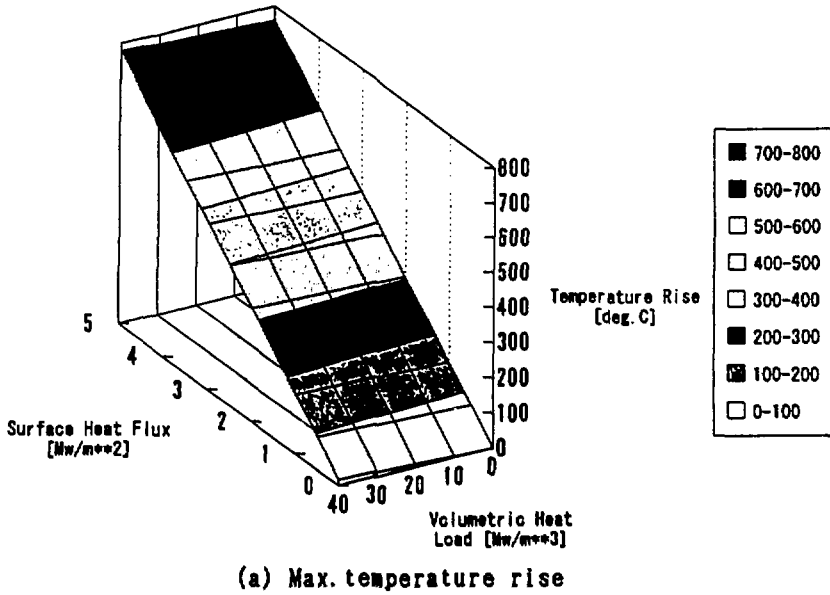


Fig. 4.3 Max. temperature rise and circumferential stress as a function of  $q_s$  and  $q_v$  for  $h_{eq} = 1 \times 10^4$  w/m<sup>2</sup>K.

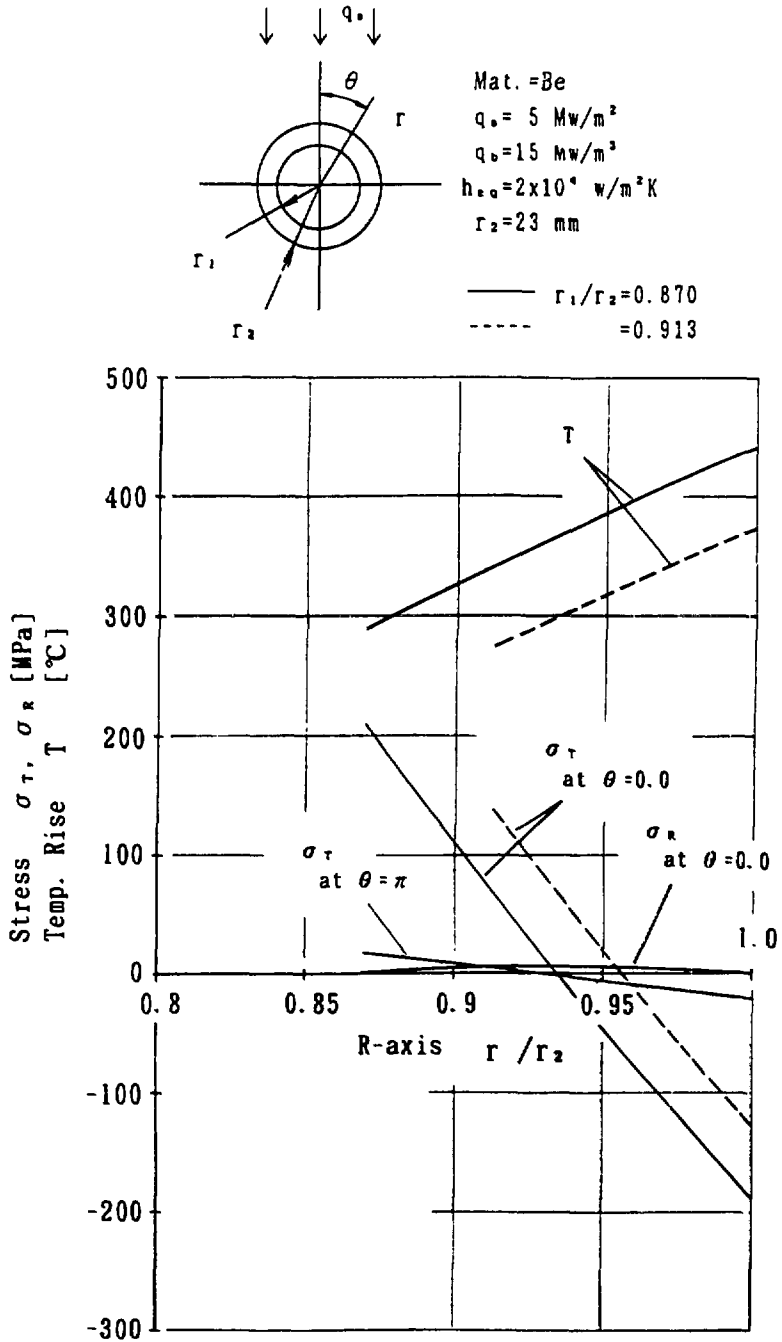


Fig. 4.4 Temperature rise and in-plane stress distributions in Be tube cooled with  $h_{eq} = 2 \times 10^4 \text{ w/m}^2\text{K}$ .

